

Operation and control of MMCs using cells with power transfer capability

Fernando Briz, Mario López, Alberto Zapico, Alberto Rodríguez, David Díaz-Reigosa
Department of Electrical Engineering, University of Oviedo, Spain
fernando@isa.uniovi.es

Abstract— Cells in conventional Modular Multilevel Converters (MMC) designs use a capacitor for energy storage. This means that the net power balance for each cell (neglecting losses) needs to be equal to zero, the MMC realizing therefore a power transfer between its DC and AC sides. This paper analyzes the design, operation and control of MMCs in which the cells have the capability to transfer (inject or drain) power. The use of such cells opens several new functionalities and uses for the MMC. On one hand, it would allow integrating elements like distributed energy storage (e.g. batteries), low-voltage/low power sources (e.g. PV) and loads at the cell level. Cells with power transfer capability can also be used connect the medium/high voltage DC and AC ports intrinsic to the MMC, with low voltage DC/AC ports at the cell level. This would result in multiport power converters, potential applications of this topology including solid state transformers (SST).¹

Keywords—Modular Multilevel Converter, MMC, Energy Storage Integration, DER Integration, Solid State Transformer

I. INTRODUCTION

The increasing penetration of renewable energies as well as the demanding requirements in terms of efficiency and reliability for their integration in the power transmission system poses a big challenge, which is expected to increase in the near future, as a significant part of the installed capacity will be connected to the distribution levels [1]. Power electronics-based technologies, like HVDC and FACTS, able to provide functionalities to the power operator such as power flow control, reduction of transmission losses and power quality improvement, will be key for this purpose [2].

The MMC was proposed one decade ago [3]-[5]. It shares several advantageous characteristics of other modular multilevel topologies, like reduced losses due to low switching frequencies and good output voltage wave shape, which leads to smaller filters and reduced voltage stress in the power devices [3]-[5]. Also, its structure based on simple cells provides scalability, which is key to achieve high voltage levels using relatively low voltage power devices. A distinguishing characteristic of the MMC is that while it provides a high voltage DC link, the distributed energy storage at the cells capacitors eliminates the need of a bulk DC capacitor, which is advantageous for safety and reliability reasons [8].

Conventional MMC designs realize a bidirectional DC-AC power conversion (see Fig. 1). The block diagram in Fig. 1-left is valid to represent either a single phase or a three-phase MMC.

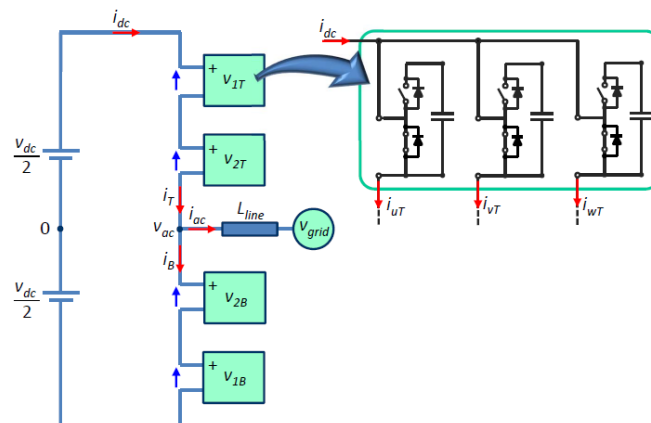


Fig. 1.- Left - Schematic representation of a conventional MMC, with the cells consisting of a half bridge. For the sake of clarity, the arm inductances are not shown. Right - Corresponding cell circuit for the case of a three-phase MMC.

The physical cells forming each arm of the power converter typically consist of a half bridge and a capacitor. For the three-phase case, each cell in Fig. 1-left physically corresponds to three individual cells (Fig. 1-right). All the analysis and discussion following assumes a three-phase AC system. However, the concepts discussed are also valid for the single-phase case. For analysis purposes, it is also assumed that the AC port of the MMC is connected to a stiff grid through a purely inductive line. Active and reactive power in the AC port are therefore controlled through the AC voltage v_{ac} . Control and modulation strategies developed for MMC are aimed to balance the power transfer between the AC and DC ports, which is done controlling the circulating current [9]-[14], as well as to balance the cell capacitor voltages [3]-[16]. Because the cells of the MMC have a limited energy storage capability, the net power balance for each cell is zero (neglecting losses), the power at the AC and DC sides of the MMC being therefore equal to each other.

It is possible to modify the MMC to transfer power at the cell level. This would provide the MMC new potential capabilities, including distributed storage [19]; integration of distributed energy resources (DER) at the cell level; multiport power converters combining the medium/high voltage DC and AC ports of the MMC with low voltage DC and AC ports; and solid state transformers. Such modification involves changes both in the cells design as well as in the control strategy. For the cells design, an electronic power converter will be needed in a general case to connect the power source transferring power

¹ This work was supported in part by the Research, Technological Development and Innovation Programs of the Spanish Ministries of Science and Innovation and of Economy and Competitiveness, under grants MICINN-10-CSD2009-

00046 and MINECO-13-ENE2013-48727-C2-1-R, and by the European Commission FP7 Large Project NMP3-LA-2013-604057, under grant UE-14-SPEED-604057.

to the cell (either injecting or draining) with the cell capacitor. Depending on the characteristics of this power source (energy storage device, renewable energy sources, ...), unidirectional or bidirectional power flow capability can be needed. Regarding the control strategies, the existing methods assume that all the cells in the MMC have identical design and operate identically. However, this is not true anymore if cells with the capability to transfer power exist.

This paper analyzes the design, operation and control of MMCs in which one or more cells have the capability to transfer (inject or drain) power. As for the conventional MMC, the control has to balance the power and provide the required AC and DC voltages at the MMC terminals. However, and contrary to the conventional MMC, the power transferred by the cells will affect to the power balance, resulting in unbalances in the cells operating point. The paper is organized as follows. The model of the conventional MMC, i.e. without power transfer at the cell level, is presented in Section II. Design and operation of cells with power transfer capability are discussed in Sections III and IV. Control strategies are discussed in Section V. Experimental results using a single phase MMC are shown in Section VI, the conclusions being presented in Section VII.

II MODEL AND OPERATION OF MMC WITH BALANCED CELLS

The MMC realizes a bidirectional DC-AC power conversion (see Fig. 1). For the analysis presented in this paper, a three-phase MMC is assumed. Complex vector notation will be used to represent the AC variables. The voltage and current vectors in the AC port of the MMC are defined by (1) and (2). The resulting top and bottom arm currents are shown in (3), the circulating current i_c being (4), whose DC component is equal to the DC current. Harmonics of the circulating current used e.g. to reduce the oscillations of the cell capacitor voltage [14,18], are not considered in the analysis following.

$$i_{ac} = \frac{2}{3} (i_u + i_v e^{j2\pi/3} + i_w e^{j4\pi/3}) \quad (1)$$

$$v_{ac} = \frac{2}{3} (v_u + v_v e^{j2\pi/3} + v_w e^{j4\pi/3}) \quad (2)$$

$$i_T = i_{dc} + \frac{i_{ac}}{2}; i_B = i_{dc} - \frac{i_{ac}}{2} \quad (3)$$

$$i_c = \frac{i_T + i_B}{2} = i_{dc} \quad (4)$$

Due to the limited energy storage capability of the cells, the power in the DC port of the MMC has to be equal to the active power in the AC port (5), * standing for complex conjugate.

$$P_{dc} = v_{dc} i_{dc} = P_{ac} = Re(v_{ac} i_{ac}^*) \quad (5)$$

It is useful to separate the MMC in Fig. 1 into its DC and AC sub-circuits, as shown in Fig. 2. For the sake of simplicity, the voltage drop in the arm inductor will be neglected. A MMC with two cells per arm ($N=2$), i.e. four cells per phase, will be considered. However, the conclusions are valid for MMCs with a different number of cells per arm (N). Assuming that the MMC is perfectly balanced (identical cells, identical operating point), the DC and AC voltages for each cell are given by (6)

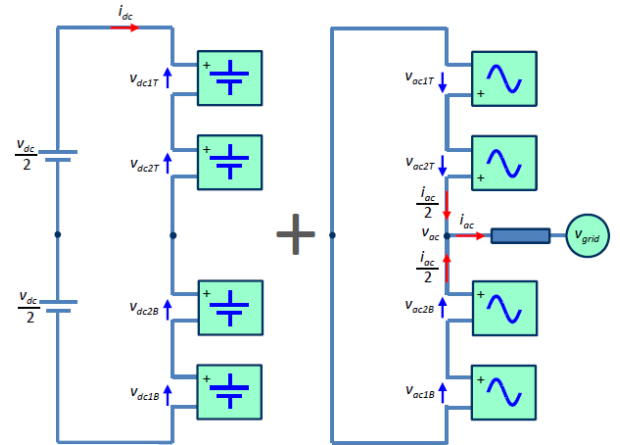


Fig. 2.- DC (left) and AC (right) sub-circuits of the MMC

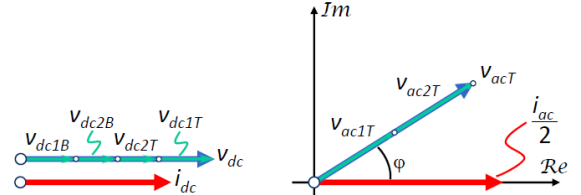


Fig. 3.- DC (left) and AC (right) voltages and currents. Only AC variables for the top arm are shown, they are the same for the bottom arm (see Fig. 2).

and (7) respectively. The overall cell voltage is therefore (8). Due to the arm inductors being neglected, the overall AC voltage for the upper and lower arms needs to be equal to v_{ac} , as they are connected in parallel (see Fig. 2-right). Consequently, the AC current splits equally between the upper and lower arms. All the cells have therefore the same DC and AC powers (9) and (10).

$$v_{dc1T} = v_{dc2T} = v_{dc1B} = v_{dc2B} = \frac{v_{dc}}{2N} = \frac{v_{dc}}{4} \quad (6)$$

$$v_{ac1T} = v_{ac2T} = v_{ac1B} = v_{ac2B} = \frac{v_{ac}}{N} = \frac{v_{ac}}{2} \quad (7)$$

$$v_{nX} = v_{acnX} + v_{dcnX} \quad \text{with } n = 1, 2 \text{ and } X = T, B \quad (8)$$

$$P_{dcnT} = P_{dcnB} = \frac{v_{dc}}{2N} i_{dc} = \frac{v_{dc}}{4} i_{dc} \quad ; n = 1, 2 \quad (9)$$

$$P_{acnT} = P_{acnB} = Re\left(\frac{v_{acT}}{N} \frac{i_{ac}^*}{2}\right) = Re\left(\frac{v_{acT}}{2} \frac{i_{ac}^*}{2}\right); n = 1, 2 \quad (10)$$

Fig. 3 graphically shows the DC and AC voltages for the MMC in Fig. 1 and 2. The AC voltages and currents are represented by complex vectors, the real axis being aligned with the AC current, where ϕ is the angle between the AC current and voltage vectors. Assumed that the voltage at the DC side of the MMC v_{dc} is constant, the MMC control has then to adjust the DC current i_{dc} to balance the power between the DC and AC ports (5). In addition, the cell capacitor voltages have to be kept at the target value. This is done by the balancing algorithms [3,4,9,12].

III. CELLS WITH POWER TRANSFER CAPABILITY

As already mentioned, it is possible to provide the MMCs the capability to transfer power at the cell level. Inserting cells with power transfer capability will produce, in general, unbalances in

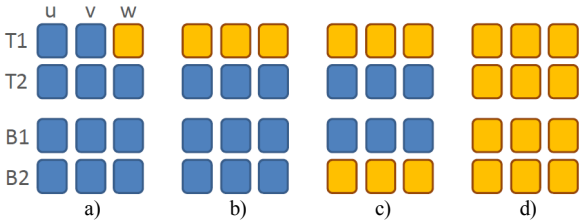
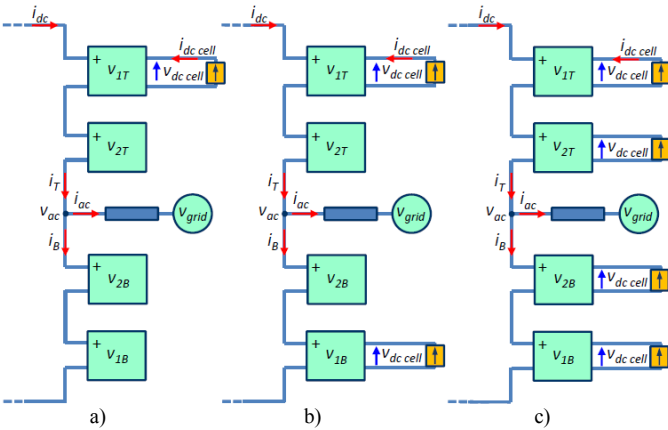
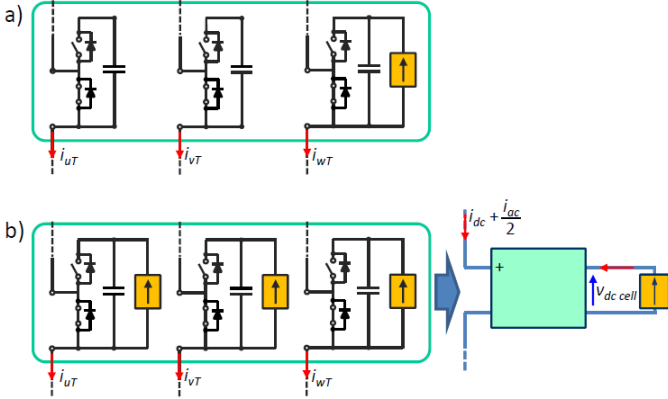
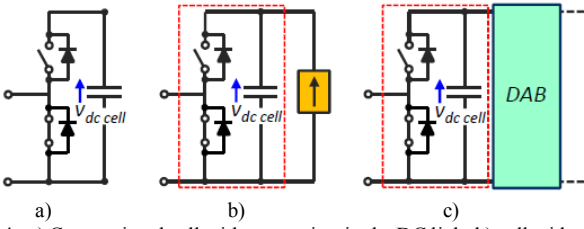


Fig. 7. Summary of MMC configurations including cells with power transfer capability. Cells in light color transfer power, cells in dark color do not (standard cells). a) Asymmetric phases (Fig. 5a); b) asymmetric top and bottom arms (Fig. 6a); c) symmetric top and bottom arms (Fig. 6b); d) fully symmetric (Fig. 6c).

the cells operation. Discussion on the design of the cells for this case, as well as the impact on the operation of the MMC, are presented in this section.

a) Cell design and power balance

When cells with power transfer capability are used, it is desirable that all the cells of the MMC have similar DC voltage $v_{dc\ cell}$, independently on whether they transfer power or not. This allows using power devices and capacitors with the same voltage ratings for all the cells. Assumed that the cells are controlled to have a capacitor voltage of $v_{dc\ cell}$, transferring power to the standard cell design in Fig. 4a can be modeled as a current source connected in parallel to the cell capacitor, as shown in Fig. 4b. It is noted however that in a practical implementation, voltage isolation between the cell capacitor and the power source will likely be needed. A current controlled dual active bridge (DAB) can be used for this purpose (Fig. 4c) [17]. This is described in section VI.

Standard MMCs require a perfect balance between the DC and AC powers (5), assumed that the losses can be neglected. Since all the cells have the same DC and AC voltages, the cells are controlled to have (ideally) the same DC and AC voltages, (6) and (7). If one or more cells transfer power, the resulting MMC power balance equation is (11), where P_{cell} is the power transferred by each cell and M is the number of cells transferring power. It is assumed that all the cells transfer a similar amount of power. This restriction is discussed latter.

$$P_{dc} + MP_{cell} = P_{ac} \quad (11)$$

b) MMC topologies using cells with power transfer capability

Examples of MMC topologies using cells with power transfer capability are shown in Fig. 5 and 6. In the example shown in Fig. 5a, only one cell in phase w transfers power, while the cells at equivalent locations in phases u and v do not. In the case shown in Fig. 5b, all the three phases include cells with power transfer capability. This results in symmetric phases, whose AC sub-circuit can be modeled as an equivalent complex vector cell (Fig. 5b-right). This is equivalent to the complex vector cells shown in Fig. 1, but now including the current source connected to the cell capacitor. Fig. 6 shows different configurations of the MMC using the complex vector cell in Fig. 5b. In the configuration shown in Fig. 6a, only cells in the upper arm transfer power. In the case shown in Fig. 6b, the same number of cells in the upper and lower arms transfer power, while in the case shown in Fig. 6c, all the cells transfer power. Fig. 7 summarizes all the cases.

Depending on the number and location of the cells transferring power (see Fig. 5 to Fig. 7), different types of asymmetries (unbalances) can occur among cells, and consequently among arms or legs of the MMC. Asymmetries cannot exist in the cells current. All the cells for each leg of the MMC have the same DC current. It is also assumed that the AC current equally splits among the top and bottom arms of each leg. In consequence, all the cells have the same DC and AC currents. Therefore, producing asymmetries in the operation of the cells will require varying their DC and/or AC voltages.

Unbalances among phases (Fig. 7a) will result in different DC voltages for the cells in phase w , eventually resulting in a DC zero sequence voltage in the AC voltage v_{ac} . The case shown in Fig. 7b produces unbalances between the DC voltage for the top and bottom arms of all the three phases, eventually resulting in a DC

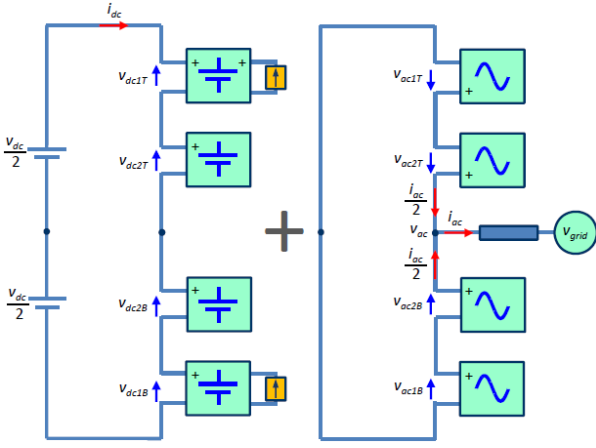


Fig. 8. - DC+cell (left) and AC (right) subcircuits of the MMC including cells with power transfer capability.

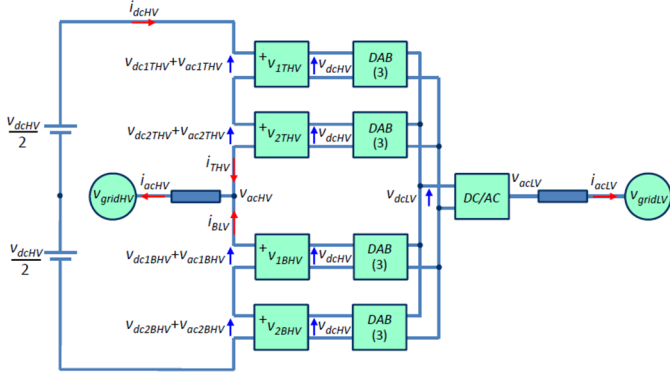


Fig. 9. - Multiport power converter using a MMC in the high voltage side and a conventional DC /AC power converter in the low voltage side.

TABLE I: TYPES OF ASYMMETRY AND EFFECTS OF CELLS WITH POWER TRANSFER CAPABILITY

Type of asymmetry	Effect on the AC port	Effect on the cells
a) Asymmetric phases (Fig. 7a)	DC zero sequence voltage	Asymmetries in the cell DC voltages
b) Symmetric phases, asymmetric arms (Fig. 7b)		
c) Symmetric arms, asymmetric cells (Fig. 7c)s	No effect	Asymmetries in the cells DC/AC voltages
d) Fully symmetric (Fig. 7d)		No effect

zero sequence component in the AC voltage v_{ac} too. In the case in Fig. 7c, top and bottom arms are symmetric, but there are unbalances among the cells in the top arm, the same occurs for the cells in the bottom arm. These unbalances can affect to the cell DC voltage, AC voltage, or both. However, as the effect is the same in the top and bottom arms, it will not have any impact on the AC voltage of the MMC v_{ac} . Finally, the case shown in Fig. 7d does not produce any type of asymmetry or effect either in the terminal voltages, arms or cells of the MMC.

Table I summarizes the different types of asymmetries produced by cells transferring power, and the impact that these can have on the MMC behavior. Cases a) and b) produce a zero sequence voltage component in the AC voltage. Whether this is tolerable or not might depend on the application. Cases c) and d) do not have any adverse effect on the terminal properties

of the MMC. However, in case c) there are differences in the operating conditions of the cells, which need to be considered for their control. This case is analyzed in more detail in the next section. Cases a), b) and d) are particular cases of c). In cases a) and b) only the cells DC voltage is varied, while case d) is an extension of case c) to all the cells.

c) MMC based multiport power converters

The use of cells with power transfer capability could potentially provide the MMC multiport capabilities. An example of this is shown in Fig. 9. It corresponds to the case shown in Fig. 7d in which all the cells transfer power. The AC and DC medium voltage ports of the MMC are connected through the cells and DABs to low voltage DC and AC ports in the right side of the figure. Other configurations are also possible, their design and analysis being the focus of ongoing research. Detailed discussion of this issue is beyond the scope of this paper.

IV. MODELING AND OPERATION OF MMC USING CELLS WITH POWER TRANSFER CAPABILITY

The use of cells with power transfer capability poses new challenges regarding the control and modulation strategies, as the methods that have been proposed are aimed to balance the operation of cells which have an identical design [3-16]. The configuration shown in Fig. 7c, (Fig. 6b) will be used for the analysis presented in this section. It has two cells per arm; cells 1T and 1B transfer power, while cells 2T and 2B do not.

a) Power balance

As already discussed in Section II, it is useful to separate the MMC in Fig. 6b into the DC and AC sub-circuits, as shown in Fig. 8. These are equivalent to the DC and AC sub-circuits shown in Fig. 2 for the conventional MMC. The power balance equation for the four cells in Fig. 8 are (12)-(15).

$$P_{dc1T} + P_{cell1T} = P_{ac1T} \quad (12)$$

$$P_{dc2T} = P_{ac2T} \quad (13)$$

$$P_{dc1B} + P_{cell1B} = P_{ac1B} \quad (14)$$

$$P_{dc2B} = P_{ac2B} \quad (15)$$

If the cells in the top and bottom arm transfer the same (or close) amount of power, then the same DC and AC voltages will exist in both arms (16). Thus, no zero sequence voltage component exists in the AC voltage of the MMC, v_{ac} . Since the AC current i_{ac} splits equally between the top and bottom arms, the power balance equation for the top arm is (17). The contribution of cells 1T and 2T are (18) and (19) respectively. Identical equations apply for the bottom arm.

In the preceding discussion, it has been assumed that all the cells transfer a similar amount of power P_{cell} (11). Significant unbalances among the power transferred by each individual cell in the cases shown in Fig. 7b-d, will result in asymmetric phases, being equivalent to Fig. 7a. The concerns previously discussed for this case would therefore apply.

$$v_{acT} = v_{acB} ; v_{dcT} = v_{dcB} \quad (16)$$

$$v_{dcT} i_{dc} + v_{dc cell} i_{dc cell} = Re \left(v_{acT} \frac{i_{ac}^*}{2} \right) \quad (17)$$

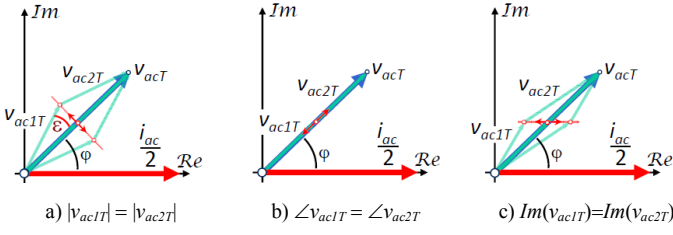


Fig. 10.- Strategies for the selection of the cell AC voltage unbalance

$$v_{dc1T}i_{dc} + v_{dc\ cell}i_{dc\ cell} = \text{Re}\left(v_{ac1T} \frac{i_{ac}^*}{2}\right) \quad (18)$$

$$v_{dc2T}i_{dc} = \text{Re}\left(v_{ac2T} \frac{i_{ac}^*}{2}\right) \quad (19)$$

b) Selection of cell voltage unbalance

The fact that cells $1T$ and $1B$ can transfer power while $2T$ and $2B$ cannot, will necessarily produce an unbalance in their operation. Since the DC and AC currents, i_{dc} and $i_{ac}/2$, are common to all the cells in the arm, the unbalance has to occur in the cell voltages v_{1T} , v_{1B} , v_{2T} , v_{2B} . This can be done unbalancing the cell DC voltage by an amount of Δv_{dc} (20)-(21), the AC voltage by an amount of Δv_{ac} (22)-(23), or both. It is noted that in all the cases (24) and (25) hold.

$$v_{dc1T} = \frac{v_{dc}}{4} + \Delta v_{dc} \quad ; \quad v_{dc1B} = v_{dc1T} \quad (20)$$

$$v_{dc2T} = \frac{v_{dc}}{4} - \Delta v_{dc} \quad ; \quad v_{dc2B} = v_{dc2T} \quad (21)$$

$$v_{ac1T} = \frac{v_{ac}}{2} + \Delta v_{ac} \quad ; \quad v_{ac1B} = v_{ac1T} \quad (22)$$

$$v_{ac2T} = \frac{v_{ac}}{2} - \Delta v_{ac} \quad ; \quad v_{ac2B} = v_{ac2T} \quad (23)$$

$$v_{dc1T} + v_{dc2T} = v_{dc1B} + v_{dc2B} = \frac{v_{dc}}{2} \quad (24)$$

$$v_{ac1T} + v_{ac2T} = v_{ac1B} + v_{ac2B} = v_{ac} \quad (25)$$

Using (12)-(25), it is possible to obtain the relationship between Δv_{dc} and Δv_{ac} and the power handled by the cells (12)-(15) and the MMC (11). For this process, it is assumed that the DC side voltage of the MMC v_{dc} and the grid voltage v_{grid} are constant (see Fig. 8), and that the active and reactive power demands from the AC port of the MMC, P_{ac} and Q_{ac} , are given. Therefore, the AC current i_{ac} and consequently the AC voltage v_{ac} , are imposed by the AC port power needs. It is also assumed that the current injected by the current source connected to the cells $1T$ and $1B$ in Fig. 8 ($i_{dc\ cell}$ in Fig. 6b) is determined by the power source connected to the cell capacitor, being therefore an independent variable. The DC current of the MMC i_{dc} needs then to be controlled to satisfy the overall power balance equation (11), similarly to the conventional MMC. In addition, Δv_{dc} and Δv_{ac} need to be selected to satisfy the balance equation of each cell.

The effect of Δv_{dc} on the power transferred by the cells can be readily calculated using (18)-(21). On the other hand, an extra degree of freedom exists for the selection of Δv_{ac} , since the AC voltage v_{ac} is a complex vector. Three different strategies for the selection of Δv_{ac} are shown in Fig. 10, which

are defined by (26), (27) and (28) respectively. It is noted that in all the cases (25) holds.

$$|v_{ac1T}| = |v_{ac2T}| \quad ; \quad \angle v_{ac1T} \neq \angle v_{ac2T} \quad (26)$$

$$\angle v_{ac1T} = \angle v_{ac2T} \quad ; \quad |v_{ac1T}| \neq |v_{ac2T}| \quad (27)$$

$$\text{Im}(v_{ac1T}) = \text{Im}(v_{ac2T}) = \text{Im}(v_{acT})/2 \quad ; \quad \text{Re}(v_{ac1T}) \neq \text{Re}(v_{ac2T}) \quad ; \quad \angle v_{ac1T} \neq \angle v_{ac2T} \quad ; \quad |v_{ac1T}| \neq |v_{ac2T}| \quad (28)$$

In the strategy defined by (26) (Fig. 10a), cells $1T$ and $2T$ have the same AC voltage magnitude. However, the phase angle of v_{ac1T} and v_{ac2T} with respect to the AC current is different. In the strategy defined by (27) (Fig. 10b), cells $1T$ and $2T$ have different AC voltage magnitude, but the same phase angle with respect to the AC current. In the strategy defined by (28) (Fig. 10c), the imaginary part of the cells $1T$ and $2T$ AC voltage is the same, but the real components $\text{Re}(v_{ac1T})$ and $\text{Re}(v_{ac2T})$ are different.

c) Discussion on the selection of Δv_{dc} and Δv_{ac} and limits of operation

The following considerations can be made regarding the selection of the voltage unbalances Δv_{dc} and Δv_{ac} to realize the power balance of the cells (11):

- Transferring power between the cells and the DC port (29) is only possible if reactive power (reactive current) circulates through the AC port of the MMC, i.e. $Q_{ac} \neq 0$.

$$P_{dc} = -P_{cell} \quad ; \quad P_{ac} = 0 \quad (29)$$

This is due to the fact that the DC current i_{dc} is common to all the cells. An unbalance of Δv_{dc} in one cell would require an unbalance of $-\Delta v_{dc}$ in another cell to maintain the DC bus voltage constant (24). As a consequence, the power injected (or drained) by the first cell would be drained (or injected) by the second cell. This power would be therefore recirculated between these two cells, with no power transfer to the DC port. Consequently, AC current (either active or reactive) is required to transfer power between the cells and the MMC.

- It is possible to transfer power between the cells and the AC port of the MMC when the DC current i_{dc} is zero, i.e.

$$P_{cell} = P_{ac} \quad ; \quad P_{dc} = 0 \quad (30)$$

The amount of power that can be transferred by the cells, P_{cell} , increases with the AC current magnitude and with the power factor ($\cos(\varphi)$) in the AC side.

- For an angle $\varphi=90^\circ$ (only reactive power is transferred through the AC port), the strategies to produce the AC voltage unbalance Δv_{ac} shown in Fig. 10a and Fig. 10c are equivalent. For $\varphi=0^\circ$ (only active power is transferred through the AC port), the strategies shown in Fig. 10b and Fig. 10c are equivalent too.
- Unbalancing the magnitude of the AC voltage (27) (Fig. 10b) does not allow to transfer power from the cells when $\varphi=90^\circ$. Unbalancing the real component of the AC voltage (28) (Fig. 10c) has the advantage of a nearly linear relationship between the level of unbalance and the power transferred by the cell.

Fig. 11 shows the power transferred by cells $1T$ (same for $1B$), and the power at the DC and AC ports of the MMC, as a function of Δv_{dc} and Δv_{ac} , for constant apparent power S_{ac} (constant $|i_{ac}|$)

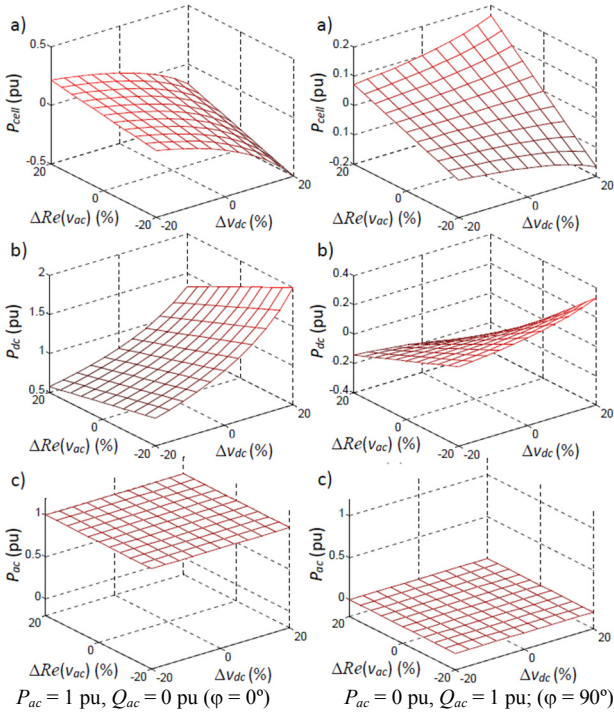


Fig. 11. - a) Cell power P_{cell} , b) DC port power P_{dc} and c) AC port power P_{ac} , as a function of $\Delta Re(v_{ac})$ and Δv_{dc} , for constant AC power S_{ac} . Left: Purely active power ($\varphi = 0^\circ$); Right: Purely reactive power ($\varphi = 90^\circ$) in the AC port. Powers are in pu of $|S_{ac}|$.

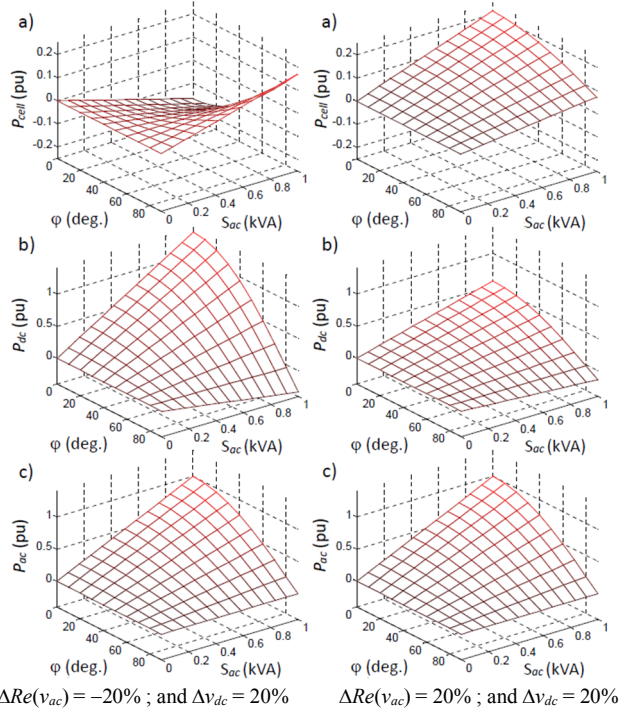


Fig. 12. - a) Cell power, b) MMC DC side power and c) MMC AC side power, as a function of apparent power S_{ac} and angle φ in the AC side, for two different unbalances $\Delta Re(v_{ac})$ and Δv_{dc} . Powers are in pu of $|S_{ac}|$.

and two different values of the angle φ . The strategy defined by (28) (Fig. 10c) was used, in which the real component of the cells AC voltage is varied, i.e. $\Delta v_{ac} = \Delta Re(v_{ac})$. Cells 2T and 2B do not transfer power (19). It is observed that for $\Delta v_{dc} =$

$\Delta Re(v_{ac}) = 0$, $P_{cell} = 0$ and $P_{dc} = P_{ac}$, which corresponds to the normal operation of the MMCs. By controlling Δv_{dc} and Δv_{ac} , it is possible to change the amount of power transferred (injected or drained) by cells 1T and 1B. It is observed in Fig. 11-right that since $P_{ac} = 0$ ($\varphi = 90^\circ$), all the power transferred by the cells goes to the DC port. In the case shown in Fig. 11-left, the power in the DC port adds to the power transferred by the cell to provide a constant power in the AC port. It is noted that in both cases, for constant Δv_{dc} , increasing $\Delta Re(v_{ac})$ increases the amount of power transferred by the cells. However, the effect of Δv_{dc} on the power transferred by the cells with constant $\Delta Re(v_{ac})$ varies with angle φ . This needs to be considered in the algorithms used to select Δv_{dc} and $\Delta Re(v_{ac})$.

Fig. 12 shows the power transferred by cell 1T (same for 1B), and the power at the DC and AC sides of the MMC, as a function of the apparent AC power (which is proportional to i_{ac}) and the angle φ in the AC side, for two different values of Δv_{dc} and Δv_{ac} . It is seen in Fig. 12b that independent of the voltage unbalance, no power is transferred by the cells when the apparent AC power is zero, i.e. $|i_{ac}| = 0$. For a given angle φ , the power transferred by cells 1T and 1B varies proportionally to S_{ac} (and therefore to $|i_{ac}|$). The variation of the power transferred by the cells with φ for constant S_{ac} is seen to change both with Δv_{dc} and Δv_{ac} .

It is concluded from the analysis presented in this subsection that the amount of power transferred (absorbed or delivered) by the cells which have power transfer capability, can be controlled by adequate selection of Δv_{dc} and Δv_{ac} . This is done without affecting to the power balance of cells which do not transfer power. This will require however the development of suitable control and modulation strategies. This is discussed in section V.

It is finally noted that in the preceding discussion the voltage drop in the arm inductors was not considered. As a result, the AC current i_{ac} equally splits between top and bottom arms. If the arm inductors are considered, then (25) does not necessary hold, i.e.:

$$v_{ac1T} + v_{ac2T} \neq v_{ac1B} + v_{ac2B} \neq v_{ac} \quad (31)$$

It is possible then to change how the current i_{ac} splits between the top and bottom arms. This would open new possibilities to produce asymmetries among the cells. Due to room limits, this case is not analyzed in this paper.

V. MODULATION AND CONTROL STRATEGIES

It has been shown that control of the power transferred by the cells is by achieved adequate selection of Δv_{dc} and Δv_{ac} . Two different methods to achieve this goal are discussed following. The first one uses a conventional control. In this case, the values for Δv_{dc} and Δv_{ac} to realize the power balance are the response of the balancing algorithms to the unbalance produced by the cells transferring power. No explicit commands for Δv_{dc} and Δv_{ac} are given. In the second method, explicit commands for Δv_{dc} and Δv_{ac} are given.

a) No explicit selection of Δv_{dc} and Δv_{ac}

Control of the MMC with cells transferring power can be realized combining the circulating current control with a sorting algorithm [14]. Power transferred by the cells naturally results

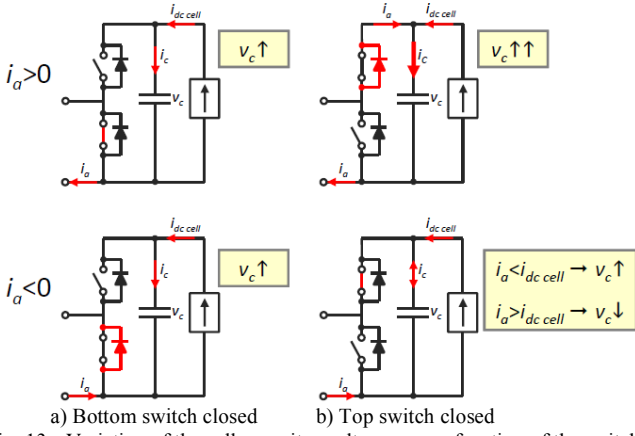


Fig. 13.- Variation of the cell capacitor voltage v_c as a function of the switches state, arm current and cell current.

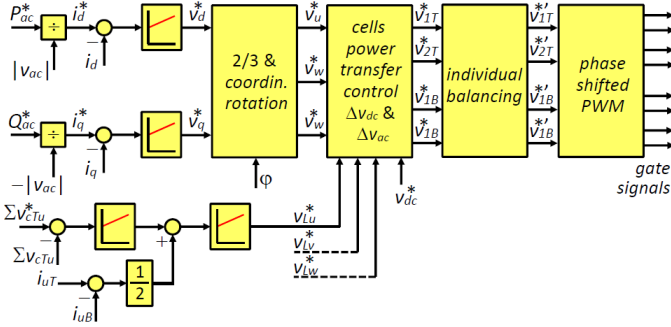


Fig. 14.- Implemented control. * stands for commanded values.

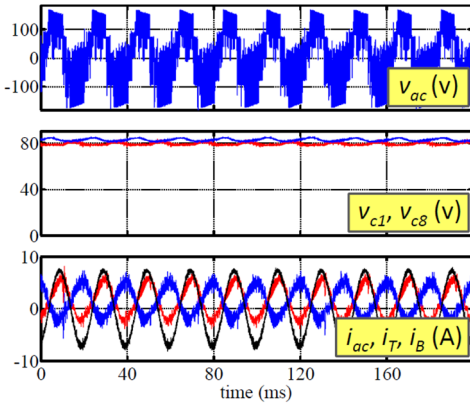


Fig. 15.- Experimental results. Top: v_{ac} ; mid: capacitor voltage for cells 1&8, bottom: i_P , i_N and i_{ac} currents.

TABLE II: EXPERIMENTAL SETUP

MMC	Power switches	600V/23A
	Cell capacitor / Arm inductance	2000uF / 1mH
	Cell voltage / DC bus voltage	80 V / 320 V
	Sampling frequency	5 kHz
DAB	Input / output voltage	12 V / 50 V
	Switching frequency	100 kHz
	Turn ratio / Leakage inductance of the transformer	N=4 / $L_k=5\mu\text{H}$

in a decrease of the circulating current (i.e. i_{dc}) and consequently of the power being transferred from the DC port.

Regarding the cell capacitor voltage balancing, sorting algorithms will naturally select the cells transferring power if needed. Fig. 13 schematically shows the variation of the cell

capacitor voltage v_c as a function of the switches state and of sign and magnitude of the arm current when a cell is transferring power. Assumed that the current source is injecting power (i.e. $i_{dc\ cell} > 0$), the cell capacitor voltage will decrease ($v_c \downarrow$) only when the top switch is closed and $i_a > i_{dc\ cell}$. In all the other cases the capacitor voltage increases ($v_c \uparrow$). The sorting algorithms will select the cells transferring accordingly. It is noted that in this case, no explicit values for Δv_{dc} and Δv_{ac} are given.

b) Explicit selection of Δv_{dc} and Δv_{ac} commands

It is possible to control the amount of power injected by the cells with power transfer capability by explicitly selecting Δv_{dc} and Δv_{ac} (see Fig. 11 and Fig. 12). In this case, control of each individual cell voltage is needed. It is noted that conventional balancing algorithms based on sorting the capacitor voltages does not have this capability [3,4,12].

Fig. 14 shows a potential implementation. The desired active and reactive power in the AC side are the inputs to the control. The “cells power transfer control” block selects the voltage unbalance Δv_{dc} and Δv_{ac} needed to realize the power transfer. With this control strategy, the power in the AC side of the MMC is maintained constant, the power transferred by the cells therefore modifying the power in the DC side. The circulating current is controlled to balance the DC power, based on the total voltage in each arm. The individual voltage reference for each cell, which includes the desired unbalance, is then obtained. Individual capacitor voltage balancing is required, a phase-shifted carrier modulation strategy is needed for this purpose [9].

VI. EXPERIMENTAL RESULTS

Preliminary experimental verification of the proposed method has been realized on an eight cell single-phase MMC. Two cells, one in the top arm and one in the bottom arm, have DAB [20,21] connected to their capacitor, therefore having the capability of transferring power (Fig. 4c). The details for the MMC and the DAB can be found in Table II. The DAB realizes a bidirectional DC/DC conversion. It uses two active full bridges interfaced through a high-frequency transformer, which provides galvanic isolation. Soft-switching operation of all the devices at nominal conditions is possible. Two complementary signals with a 50% duty cycle were used to control each full bridge. The power flow is controlled by varying the phase-shift between these signals. Feedback control with a PI regulator was used to control the current injected to the cell by the DAB.

The control strategy described in Section V-a was used to control the MMC. Therefore, no explicit commands for Δv_{dc} and Δv_{ac} are given, instead they result from the reaction of the control and sorting algorithms to the power transferred by the cells. Fig. 15 shows various wave shapes during the normal operation of the MMC. Fig. 16 shows the DC component as well as the magnitude and phase of the AC (50 Hz) component of the cells voltage for the top arm, both for the case when the cells do not transfer power (conventional MMC) and when one cell per arm transfers power. Bottom arm behaves similarly. Two different cases of power transferred by the cells P_{cell} of 10% and 20% of the AC power P_{ac} are shown in Fig. 16a and Fig. 16b respectively. Fig. 16-right shows the power in the DC

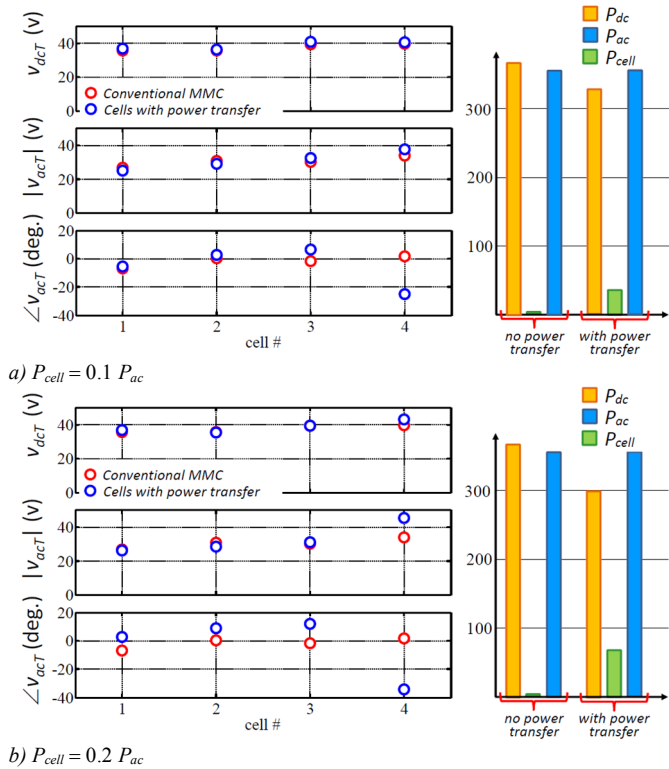


Fig. 16.- Experimental results. Left: DC and AC component of the cell voltage (only results for cells #1 to #4 shown); right: DC, AC and cells power without/with cell power transfer, for two different values of the power transferred by the cells. P_{ac} remains constant when the cells transfer power.

and AC sides of the MMC, as well as the power transferred by the cells. As already mentioned, the MMC is controlled to maintain constant the power in the AC side, meaning that power transferred by the cells affect to the DC side of the converter.

It is observed from Fig. 16a and 16b that the DC component of the cells voltage barely changes. Larger changes are observed in the magnitude of the AC voltage of cell #4 v_{ac4T} . However, the most noticeable changes in the cell voltage occur in the angle $\angle v_{ac4T}$. This would correspond to the case shown in Fig. 10a. It is noted that Δv_{dc} and Δv_{ac} are not explicitly given, the use of the strategy shown in Fig. 14 would allow to optimize their use. Implementation of this strategy is in progress.

VII. CONCLUSIONS

This paper analyzes the design and control of MMCs in which the cells have the capability to transfer (inject or absorb) power. The use of such cells provides to the MMC new functionalities, like distributed energy storage and connection of low-voltage/low power sources and loads at the cell level. The concept can also be used to realize different types of multiport power converters, including SSTs. Cell design, operational limits and control strategies have been presented and discussed. In the proposed cell design, a DAB has been used to transfer power providing galvanic isolation. It has been shown it is possible to control the amount of power injected by the cells by adequate selection of the cell DC and AC voltages. This can be realized using conventional control algorithms for the MMC. However, design of control algorithms to optimize the selection

of Δv_{dc} and Δv_{ac} is desirable and is the focus of ongoing research. The proposed concepts have been confirmed experimentally.

REFERENCES

- [1] Gemell, B.; Dorn, J.; Retzmann, D.; Soerangr, D., "Prospects of multilevel VSC technologies for power transmission," Transmission and Distribution Conference and Exposition, 2008. T&D. IEEE/PES, vol., no., pp.1,16, 21-24 April 2008
- [2] Xiao-Ping Zhang, Christian Rehtanz, Bikash Pal, Flexible AC Transmission Systems: Modeling and Control. Springer, 2012
- [3] A. Lesnicar, and R. Marquardt: An Innovative Modular Multilevel Converter Topology Suitable for a Wide Power Range, IEEE PowerTech Conference, Bologna, Italy, June 23-26, 2003.
- [4] M. Glinka and R. Marquardt: A New AC/AC Multilevel Converter Family, IEEE Trans. on Industrial Electronics, vol. 52, no. 3, June 2005.
- [5] A. Lesnicar, and R. Marquardt: A new modular voltage source inverter topology, EPE 2003, Toulouse, France, September 2-4, 2003.
- [6] Pefitsis, D.; Tolstoy, G.; Antonopoulos, A.; Rabkowski, J.; Lim, Jang-Kwon; Bakowski, M.; Angquist, L.; Nee, H-P, "High-power modular multilevel converters with SiC JFETs," Energy Conversion Congress and Exposition (ECCE), 2010 IEEEpp.2148-155, 12-16 Sept. 2010.
- [7] J. Rodriguez, J.-S. Lai, and F. Z. Peng, "Multilevel inverters: A survey of topologies, controls, and applications," IEEE Trans. Ind. Electron., vol. 49, no. 4, pp. 724-738, Aug. 2002.
- [8] Rohner, S.; Bernet, S.; Hiller, M.; Sommer, R.; "Analysis and Simulation of a 6 kV, 6 MVA Modular Multilevel Converter," 35th Annual Conf. of IEEE Ind. Elect.. IECON '09., pp. 225-230, 3-5 Nov. 2009.
- [9] Hagiwara, M.; Akagi, H.; "Control and Experiment of Pulsewidth-Modulated Modular Multilevel Converters," Power Electronics, IEEE Trans. on, vol.24, no.7, pp.1737-1746, July 2009.
- [10] Akagi, H., "Classification, Terminology, and Application of the Modular Multilevel Cascade Converter (MMCC)," IEEE Trans. On Power Elect., vol.26, no.11, pp.3119-3130, Nov. 2011.
- [11] Hagiwara, M.; Maeda, R.; Akagi, H.; "Control and Analysis of the Modular Multilevel Cascade Converter Based on Double-Star Chopper-Cells (MMCC-DSCC)," IEEE Trans. On Power Elect., vol.26, no.6, pp.1649-1658, June 2011.
- [12] Antonopoulos, A.; Angquist, L.; Nee, H.-P.; "On dynamics and voltage control of the Modular Multilevel Converter," 13th European Conference on Power Elect. and Appl., 2009. EPE '09. pp.1-10, 8-10 Sept. 2009.
- [13] Perez, M.A.; Lizana F, R.; Rodriguez, J., "Decoupled current control of modular multilevel converter for HVDC applications," 2012 IEEE Int. Symposium on Ind. Elect. (ISIE), pp.1979-1984, 28-31 May 2012.
- [14] Jae-Jung Jung; Hak-Jun Lee; Seung-Ki Sul, "Control strategy for improved dynamic performance of variable-speed drives with the Modular Multilevel Converter," Energy Conversion Congress and Exposition (ECCE), 2013 IEEE, pp.1481-1488, 15-19 Sept. 2013.
- [15] Saedifard, M.; Irvani, R., "Dynamic Performance of a Modular Multilevel Back-to-Back HVDC System," Power Delivery, IEEE Trans. on, vol.25, no.4, pp.2903-2912, Oct. 2010.
- [16] Rohner, S.; Bernet, S.; Hiller, M.; Sommer, R.; "Pulse width modulation scheme for the Modular Multilevel Converter," 13th European Conference on Power Electronics and Appl. EPE '09. pp.1-10, 8-10 Sept. 2009.
- [17] Zhao, T.; Wang, G.; Bhattacharya, S.; Huang, A Q., "Voltage and Power Balance Control for a Cascaded H-Bridge Converter-Based Solid-State Transformer," IEEE Trans. on Power Elect., vol.28, no.4, pp.1523-1532, April 2013
- [18] Hagiwara, M.; Hasegawa, I.; Akagi, H., "Start-Up and Low-Speed Operation of an Electric Motor Driven by a Modular Multilevel Cascade Inverter," IEEE Trans. on Ind. Appl., vol.49, no.4, pp.1556,1565, July-Aug. 2013
- [19] Vasiladiotis, M.; Rufer, A., "Analysis and Control of Modular Multilevel Converters With Integrated Battery Energy Storage," Power Electronics, IEEE Trans. on, vol.30, no.1, pp.163,175, Jan. 2015
- [20] DeDoncker, R. W.; Divan, R. W.; Kheraluwala, M.H., "A three-phase soft-switched high power-density dc/dc converter for high -power applications". IEEE Trans. on Ind. Appl., vol. 27, p. 63-73. Jan. 1991.
- [21] Rodriguez, A.; Vazquez, A.; Lamar, D.G.; Hernando, M.M.; Sebastian, J., "Different Purpose Design Strategies and Techniques to Improve the Performance of a Dual Active Bridge With Phase-Shift Control," IEEE Trans. on Power Elect., vol.30, no.2, pp.790,804, Feb. 2